Geomechanics and Engineering, *Vol. 38, No. 1 (2024) 1-13*
https://doi.org/10.12989/gae.2024.38.1.001

Deformation characteristics of surrounding rock in the intersection area between main tunnel and construction adit of the Xianglushan tunnel

Yunjuan Chen[1,2a], Mengyue Liu*[2], Fuqiang Yin[3b], Lewen Zhang[4c], Jing Wu[4d] and Jinrui Li[4e]

[1]*Key Laboratory of Building Structural Retrofitting and Underground Space Engineering (Shandong Jianzhu University), Ministry of Education, Jinan 250101, China*
[2]*School of Civil Engineering, Shandong Jianzhu University, Jinan 250101, China*
[3]*Shandong Provincial Institute of Land Surveying and Mapping, Jinan 250102, China*
[4]*Institute of Marine Science and Technology, Shandong University, Qingdao 266237, Shandong, China*

(*Received October 25, 2023, Revised April 10, 2024, Accepted June 17, 2024*)

Abstract. The construction adit plays a pivotal role in enhancing the working face during the excavation of long-distance and deep hydraulic tunnels. However, the intersection zone between the main tunnel and the construction adit exhibits more intricate deformation patterns in surrounding rock, posing a significant threat to stability during excavation. Taking the Xianglushan tunnel in Yunnan Province, China, as a case study, the FLAC3D software is employed to simulate the excavation process at the intersection. The simulation results are verified combined with the field deformation monitoring results, and the spatial distribution of tunnel rock deformation in the intersection area are analyzed. Five excavation conditions with different intersection angles are simulated, and the surrounding rock deformation of the tunnel intersection area with different intersection angles is analyzed, and its influence range is discussed. The results show that: (1) The surrounding rock deformation in the intersection area increases rapidly during the tunnel excavation. With the increase of construction distance, the deformation of intersection area is gradually stable. (2) The deformation distribution of the tunnel rock is uneven, and the deformation of main tunnel near the intersection area is larger than that far away from the intersection area. (3) With the increase of the intersection angle, the surrounding rock deformation of the tunnel intersection and its influence range decreases gradually. The research results have certain guiding significance for the construction safety of the tunnel intersection area.

Keywords: deformation characteristics; field monitoring; intersection angle; intersection area; numerical simulation

1. Introduction

The excavation of deep and long-distance hydraulic tunnel is very difficult (Fan *et al*. 2021). To improve construction efficiency and construction conditions of ventilation and drainage, different construction adits are set up in the process of the hydraulic tunnel construction. However, the spatial structure of the tunnel intersection area between the main tunnel and construction adit is very complex (Hsiao *et al*. 2009, Liu *et al*. 2017, Dong *et al*. 2020, Chortis and kavvadas 2021). The stress state and deformation at the intersection area are three-dimensional (Gercek 1986). The excavation of the tunnel will cause stress redistribution and great deformation of the supporting structure and rock. The stability of the intersection area will be seriously affected during the tunnel construction. The disturbance of excavation is likely to cause lining cracking at the intersection and the collapse of the tunnel (Liang *et al*. 2020). Therefore, it is very necessary and meaningful to study and analyze the deformation characteristics of surrounding rock in the intersection area between the main tunnel and construction adit (Elkadi and Huisman 2002, Johnson and Leven 1977).

In the previous studies on the behavior of the surrounding rock in the tunnel intersection area, the traditional three-dimensional photo-elasticity method was widely used to determine the stress (Budarapu 2014, 2015, Sudhir Sastry 2014, 2015, Riely 1964). In recent years, numerical simulation technology is gradually matured (Nawel and Salah 2015, Chen *et al*. 2022, Shi *et al*. 2022). The simulation methods have been used in the deformation and mechanical analysis of tunnel excavation (Li *et al*. 2021, Song *et al*. 2021, Liu *et al*. 2011, Shi *et al*. 2015, Jiang *et al*. 2019). Researchers all over the world have also widely used simulation methods to study the stress and deformation distribution in the tunnel intersection area (Chen and Tseng 2010). Liu and Wang (2010) simulated the three-dimensional excavation and support of tunnel intersection area under four working conditions and analyzed the deformation and stress using Ansys software.

*Corresponding author, Master Candidate
E-mail: liuyuximeng@163.com
[a]Associate Professor
E-mail: chenyunjuan@sdjzu.edu.cn
[b]Engineer
E-mail: yinfuqiang@shandong.cn
[c]Professor
E-mail: lewenzhang@sdu.edu.cn
[d]Associate Professor
E-mail: wujing9516@163.com
[e]Graduate Student
E-mail: 18860652919@163.com

ISSN: 2005-307X (Print), 2092-6219 (Online)

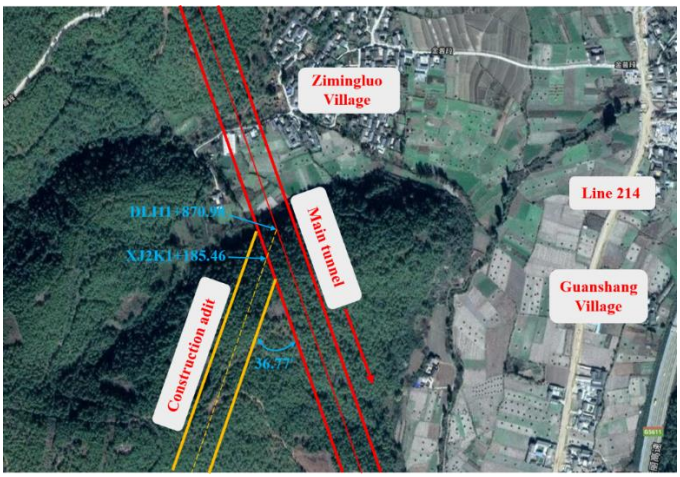

Fig. 1 Study area

Lin *et al.* (2013) established a three-dimensional numerical model of tunnel intersections between the tailrace tunnel and hydropower station to investigate the distributions of plastic zones, stresses and deformations. Li *et al.* (2016) analyzed the deformation and mechanical characteristics of the intersection area between construction tunnel and subway station tunnel to discuss the influence scope of deformation in the intersection area using the Midas-GTS software. Liu *et al.* (2017) studied the deformation behavior of the intersection area when the intersection angle is 90°, and put forward the principles of detection and reinforcement in the intersection area. Joneidi *et al.* (2019) evaluated the influence of shallow tunnel intersection area on ground deformation at different construction stages by field deformation monitoring and numerical simulation method.

However, the existing literature mainly studies the spatial intersection structure composed of highway or railway main tunnel and cross passage. There are few studies on the deformation characteristics of rock in the intersection area of the hydraulic tunnel. The spatial structure of the intersection area between the main tunnel and the construction adit is relatively complex, with a large free face. The excavation of the main tunnel in the intersection area inevitably breaks the stable state of the surrounding rock mass, releasing and redistributing the stress of the surrounding rock and support structure in the intersection area, resulting in more serious deformation of the surrounding rock. This poses significant challenges to the excavation construction, rock support reinforcement, and monitoring and measurement of the intersection area. There are many factors that affect the deformation of the surrounding rock in the intersection area of the main tunnel and the construction support tunnel in practical engineering. The intersection angle between the main tunnel and the construction adit, the distance to the intersection center, the depth of the tunnel, the grade of the surrounding rock, and the excavation method all have a significant impact on the deformation of the surrounding rock in the intersection area.

It can be seen that the deformation of the surrounding rock in the intersection area is a very complex problem with many uncertain factors. Therefore, in order to ensure construction safety and tunnel stability in the intersection area, it is of great practical significance to study and analyze the deformation characteristics and influencing factors of the surrounding rock in the intersection area of the main tunnel and the construction adit.

In this study, the deformation Characteristics of Surrounding Rock in the Intersection Area between Main Tunnel and Construction Adit of the Xianglushan Tunnel is studied. Chapter 2 introduced the engineering geology of Xiangrushan Tunnel and the overview of the study area. Chapter 3 provides a detailed introduction to the numerical simulation method, including model establishment and basic assumptions, parameter selection and boundary condition setting, simulation excavation steps, etc. Chapter 4 verifies the accuracy of numerical simulation through on-site monitoring results. Chapter 5 studied the influence of intersection angle on the deformation of surrounding rock in the intersection and discussed the influence range of intersection area with different intersection angles. Chapter 6 is the conclusion and prospect of this paper.

2. Engineering background

Xianglushan tunnel is the longest deep-buried tunnel of the water diversion project in central Yunnan Province, China. It is located at the head of Dali section I. The length of the Xianglushan tunnel is about 62.596 km. The engineering geological and hydrogeological conditions are very complex. The 2# construction adit of Xianglushan tunnel is located at the west of Guanshang Village, Lijiang City. The intersection angle between the 2# construction tunnel and the main tunnel is 36.77°. The relative positions of the main tunnel and the 2# construction adit are shown in Fig. 1.

2.1 Landform

The topography of the construction section I of Dali of the Dianzhong Water Diversion Project is controlled by the structure, with mountains and major water systems running in a nearly north-south direction, with mountains, deep valleys, and basins distributed alternately. The terrain along the tunnel is steep and continuous, with a mountain top height of

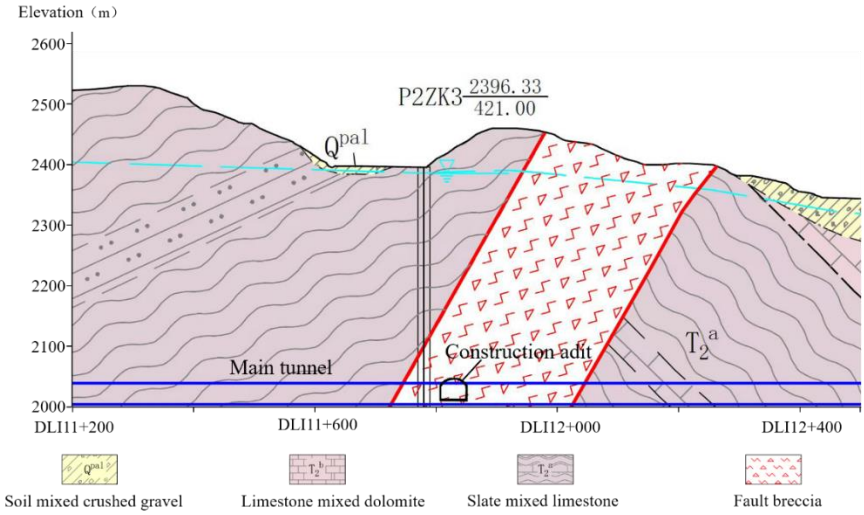

Fig. 2 The geological section

generally 2380-286 0 m. The east side is 1.5-2 km parallel to the Daluojing gully, with an overall direction of NW. The bottom elevation of the gully is generally 1840-2400 m, and the flow is significantly affected by seasonal rainfall replenishment; In addition, the final section of the tunnel is distributed in the Baihanchang 19 River Channel Valley, with an elevation of generally 2280-2400 meters.

2.2 Stratigraphic lithology

The tunnel mileage DL I 0+500- DL I 4+000 is the beginning of the section. The rock types of the strata crossed by the tunnel are mainly sericite quartz schist, sericite schist, marble interbedded with limestone, and the hanging wall of the last section F9 is sericite schist interbedded with limestone of the Ranjiawan Formation. Sericite quartz schist, marble, and limestone belong to medium hard to hard rocks, with relatively complete rock masses. The surrounding rocks are mainly Class III, and the conditions for cave formation are good. The integrity of the surrounding rock in the core section of the Shigu syncline is deviated and rich in water, belonging to Class IV surrounding rock with poor conditions for cave formation. The rock quality of the sericite schist cave section is relatively soft and has poor integrity.

The tunnel mileage D I4+000- DL I11+600 is in the middle of the section. The rock types of the strata crossed by the tunnel are mainly the middle Triassic epidote schist, epidote quartz schist interbedded with chlorite schist, quartz sandstone, etc. The overall surrounding rock is mainly of Class IV, with a small amount of Class III, and the overall conditions for cave formation are poor.

The tunnel mileage DL I 11+600- DL I 13+900 is the tail end of the section. The tunnel mainly passes through the Baihanchang valley, and the lithology is mainly composed of middle Triassic schist interbedded with limestone, as well as upper Triassic sand and mudstone interbedded with schist, with thin strip limestone and fractured rock mass. The surrounding rock is mainly of Class IV and V, and the conditions for tunnel formation are poor. The stability of the surrounding rock is prominent.

2.3 Geological structure

This section of the tunnel is located within two tertiary structural units, the Dongwang Judian Fold Bundle and the Sanba Fold Bundle; Passing through the Dalishu Fault and the Longpan-Qiaohou Fault Zone in sequence, branching faults. The research area is active in new tectonic movements, and the tunnel section is located in the strong uplift area of Zhongdian Yulong Snow Mountain and the Zhongdian Lijiang Dali seismic zone. The maximum impact intensity of historical earthquakes on the tunnel and construction support tunnels is VIII degrees.

2.4 Hydrological and meteorological conditions

The main surface water systems in the route area are Daluojinggou, Baihanchang Dagou, and Baihanchang Reservoir. The climate type of the area where the construction of Section I of Dali through belongs to the low latitude plateau monsoon climate, characterized by small temperature differences throughout the four seasons, insignificant changes, distinct dry and wet seasons, significant vertical differences, and obvious three-dimensional climate. The rainfall in the watershed is affected by the monsoon, with warm and less rainfall in the dry season and warm and rainy in the rainy season. However, the average annual precipitation in the basin is relatively low, lower than the provincial average level, and it belongs to an arid and water deficient area.

2.5 Overview of the study area

Fig. 2 shows the geological section of the study area. The depth of the intersection is 349 m. The intersection area between the main tunnel and construction adit is located in the West Branch (f10-1) of the Longpan-Qiaohou fault, which is mainly the geological formations composed of epidote schist in the Triassic period. The structural rock in the fault zone is mainly breccia, intercalated with banded silty rock and granulite. The rock mass is broken and the lithology is soft. Therefore, it is determined as a special poor class-V

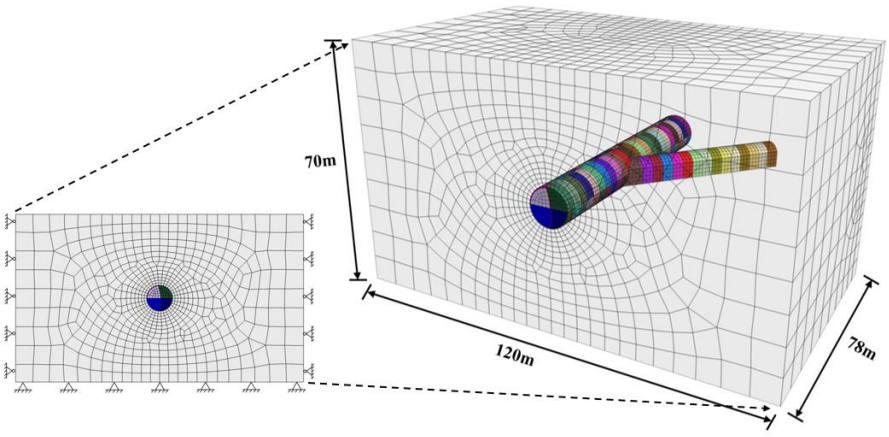

Fig. 3 The three-dimensional numerical model

surrounding rock, the surrounding rock class refers to the Engineering Rock Classification Standard of China. The stability ability of the surrounding rock is very poor. Therefore, the tunnel mainly has the problems of surrounding rock stability and extrusion deformation of weak structural rock, and there is a high risk of loose surrounding rock falling and collapsing during construction.

The section shape of the construction adit is a straight wall arch, with a width of 6.4 m and a height of 6.5 m. The section shape of the main tunnel is round with a diameter of 10.9 m. The diameter ratio between the construction adit and the main tunnel is approximately 0.60. Since the intersection area is in the fracture zone and the excavation span is large, the main tunnel is excavated by the CRD method.

3. Numerical simulation of main tunnel construction in the intersection area

3.1 Numerical model and basic assumption

Based on the engineering geology of the study area, the three-dimensional numerical model of the intersection area between the main tunnel and construction adit is established. Fig. 3 shows the perspective view of the numerical model. Considering the influence of boundary effect is a necessary process to determine the size of numerical model. The distance between the boundary of the numerical model and the sidewall of the main tunnel shall be set at least three times the diameter of the main tunnel for improving the accuracy of simulation results. Therefore, the total length of the numerical model is 120 m, and the total height of the numerical model is 70 m. To fully reflect the influence of the tunnel excavation process on the tunnel deformation, the width of the numerical model is set as 78 m. The included angle between the main tunnel and construction adit is set as 36.8˚ according to the actual situation of the engineering. The primary support and temporary support of the tunnel are composed of the universal beam, reinforcement mesh, and concrete. The primary support thickness of the main tunnel is set as 250 mm and that of the construction adit is set as 200mm. The numerical model has a total of 71217 zones and 45777 nodes. To simulate the boundary conditions, displacement constraints are applied to the front, back, left, right and bottom of the model, so these borders are fixed borders and the top borders are free borders. The assumptions are as follows:

(1) When assigning the surrounding rock parameters, it is assumed that the surrounding rock is a uniform, continuous and isotropic medium with basic lithology, without considering the influence of joints and cracks in the surrounding rock.

(2) Due to the large buried depth of the tunnel, it is impossible to simulate all the overlying rock mass above the tunnel, so it is assumed that the vertical stress is the weight of the overlying rock mass, regardless of the difference in shape and mechanical properties of the overlying rock mass, and the uniform load is applied to simulate the formation pressure at the upper boundary of the model.

(3) Assuming that the structural stress distribution in the intersection area is uniform, the maximum lateral pressure coefficient of horizontal principal stress is 1.0.

(4) This model only considers the role of initial support and temporary support, and does not consider the supporting role of secondary lining.

(5) Do not consider the role of groundwater.

It is really essential to select an appropriate constitutive model for simulating the mechanical properties of support structure and rock mass. Due to the special properties and deformation mechanism of rock in the fracture zone, the Mohr-Coulomb model is selected to simulate the properties of rock mass. Moreover, the elastic model is selected to describe the properties of primary support and temporary support.

In the numerical analysis of engineering, the selection of calculation parameters has a significant impact on the calculation results. According to the geological survey report and construction scheme of the actual project, the calculation parameters of rock, primary support, and temporary support are determined. The numerical simulation parameters are

Table 1 The numerical simulation parameters

material name	Density (kN/m^3)	Poisson's ratio	Young's modulus (GPa)	Cohesion (MPa)	Friction angle (°)
rocks	23.8	0.24	6.3	0.38	32
primary support	26.4	0.2	33.2	/	/
temporary support	26.4	0.2	33.2	/	/

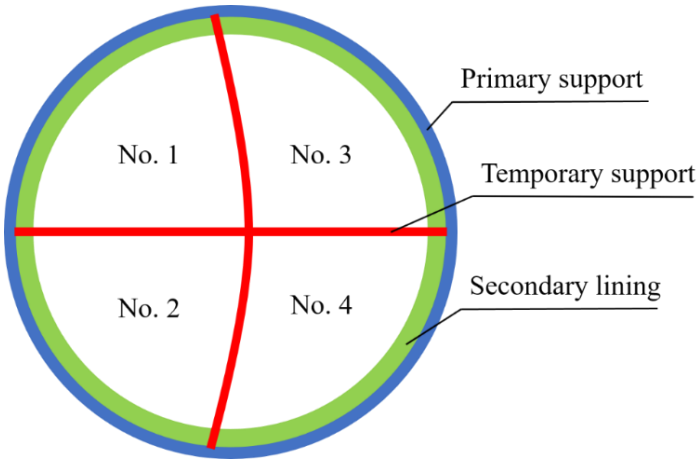

Fig. 4 The excavation sequence of the main tunnel

shown in Table 1. For the purpose of simplifying the calculation, Young's modulus of universal beam and reinforcement mesh is transformed into concrete for equivalent substitution according to the strength equivalence principle.

3.2 Construction steps simulation

The tunnel construction process adopts the method of step-by-step simulation. As the excavation of the construction adit is an advanced project, the excavation simulation of the construction adit is not included in the construction steps. The bench method is used to excavate the intersection area from top to bottom after the construction tunnel is excavated. The excavation process of the intersection area is simulated in steps 1-14. The main tunnel is excavated simultaneously along with the upstream and downstream directions of the main tunnel by the CRD method. The excavation process of the main tunnel is simulated in steps 15-104. The excavation sequence of the main tunnel is shown in Fig. 4. The CRD method divides the main tunnel section into four parts. Part No.1 is excavated by weak blasting. After the face is closed by spraying 8cm thick concrete, the initial support and temporary support of part No.1 are constructed in time. After 4 m behind part No.1, part No.2 is excavated by weak blasting. Then, the temporary support and temporary support around the heading of part No.2 are constructed. Part No.3 is excavated after 8m behind part No.2 and the excavation and support steps are the same as that of part No.1. Part No.4 is excavated after 4m behind part No.3 and the excavation and support steps are the same as that of part No.2. The excavation length of each construction step is 2m. In this simulation, the temporary support is removed after the excavation of part No. 1 is 16m. The removal length of each temporary support is set as 2m, and the one sectional removal of temporary support is taken as one separate construction step. Therefore, a total of 104 construction steps are used in this simulation, and a calculation is carried out after each construction step is completed.

4. Verification of simulation results

To ensure the construction safety of the tunnel during excavation, it is essential to monitor the deformation of tunnel in the field (Li *et al.* 2019, Luo *et al.* 2017). The field monitoring of tunnel deformation mainly includes the settlement of the tunnel vault and the horizontal displacement of tunnel sidewall. Leica TS09plus total station and laser reflector are mainly used to obtain more accurate monitoring results in this field monitoring. As shown in Fig. 5, the monitoring section is set every 10m of tunnel. Moreover, three monitoring points are set for each monitoring section to fix the laser reflector at the position of each monitoring point. The frequency of monitoring is determined according to the distance between the monitoring section and the excavation surface. The deformation of tunnel is monitored once a day when the distance to the excavation surface is less than twice the diameter of the main tunnel. The deformation of tunnel is monitored every two days when the distance to the excavation surface is larger than twice the diameter of the main tunnel. Each monitoring section is monitored continuously for 90 days. The monitoring accuracy is limited to 0.1 mm.

To verify the numerical simulation results, the vault settlement of the intersection center section is compared with the field monitoring data, as shown in Fig. 6. Due to the existence of the intersection, only one arch waist monitoring point is arranged at the intersection center section of the main tunnel, and the horizontal displacement on both sides of the intersection center section cannot be monitored. Therefore, the

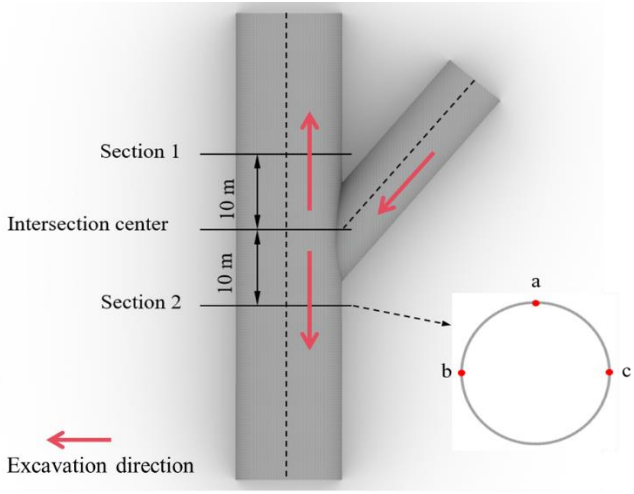

Fig. 5 Site monitoring section and monitoring point

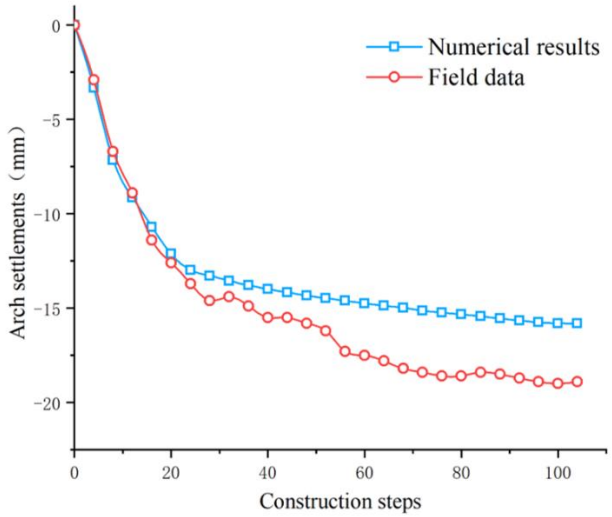

Fig. 6 Variation curve of vault settlement with construction steps

horizontal displacement of the Section 1 is selected and compares with the field monitoring data, as shown in Figure 7. As the field monitoring data is time-based, it is sorted out to match it with the simulated construction steps according to the field construction records.

It can be found out from Fig. 6 that the excavation of the tunnel intersection area has an obvious effect on the settlement of the arch crown of the main tunnel. When the tunnel intersection area is constructed, the vault settlement at the tunnel intersection center increases significantly. During the subsequent construction of the main tunnel, the vault settlement at the intersection center still increases, but the settlement rate decreases gradually. Finally the vault settlement tends to be stable. It can be found out from Fig. 7 that the excavation of the tunnel intersection area has little effect on the horizontal displacement of the main tunnel. After the excavation of section 1, the clearance convergence of tunnel increases gradually. Then, the excavation of the main tunnel has little effect on the tunnel clearance convergence, and finally, the horizontal displacement tends to be stable.

Comparing the calculation results with the field monitoring data, it can be found out that the deformation value of the field monitoring is larger than that of the numerical simulation, that is because the construction process and geological conditions of actual engineering are more complex. However, the trend of the calculation results is consistent with the monitoring data of field, which shows that the numerical simulation results accord with the actual deformation law.

5. Analysis of simulation results

5.1 Spatial distribution characteristics of deformation

To study the spatial distribution of tunnel rock deformation in the intersection area, 20 monitoring points are set along the axial direction of the main tunnel. The position of the monitoring points is shown in Fig. 8. The vertical displacement of monitoring points at the top and bottom sides of the tunnel is extracted. Then, the vertical displacement change curve along

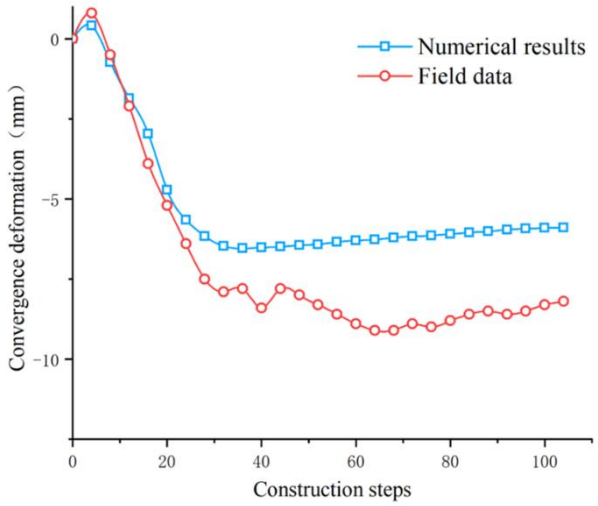

Fig. 7 Variation curve of clearance convergence with construction steps

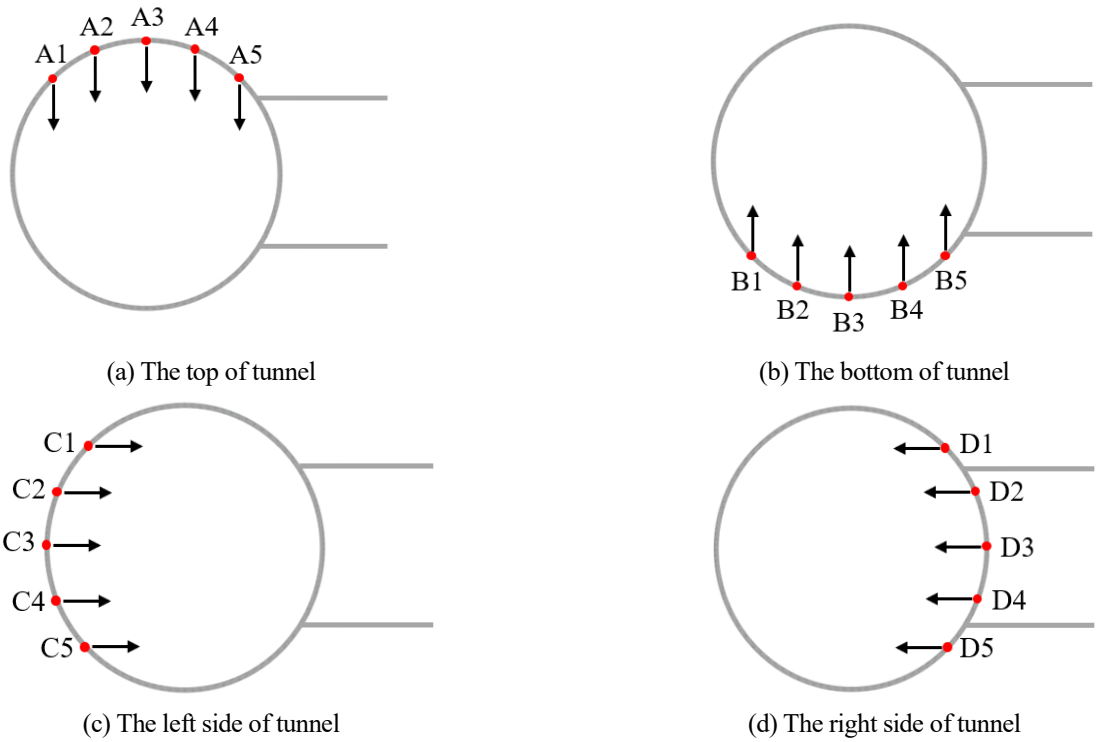

(a) The top of tunnel

(b) The bottom of tunnel

(c) The left side of tunnel

(d) The right side of tunnel

Fig. 8 Layout of monitoring points

the tunnel axis is established, as shown in Fig. 9. The positive value represents uplift, and the negative value represents settlement. The horizontal displacement of the monitoring points on the left and right sides of the tunnel is extracted. Then the horizontal displacement change curve along the tunnel axis is established, as shown in Fig. 10. The positive value represents convergence, and the negative value represents expansion.

It can be found out from Fig. 9(a), that the vertical displacement distribution at the top of the tunnel is uneven due to the existence of the intersection area. When the distance to the intersection center section is the same, the vertical displacement at the acute angle side is greater than that at the obtuse angle side. On the top of the tunnel, the vertical displacement of monitoring points at different locations is different. The horizontal displacement at monitoring point A1 is the smallest, and the curve of it is almost flat. The vertical displacement of monitoring points A3 and A4 are larger than that of monitoring points A1 and A2. the vertical displacement of monitoring point A5 changes the most. It can be concluded that the closer the monitoring point is to the intersection area, the larger the vertical displacement is. The maximum vertical

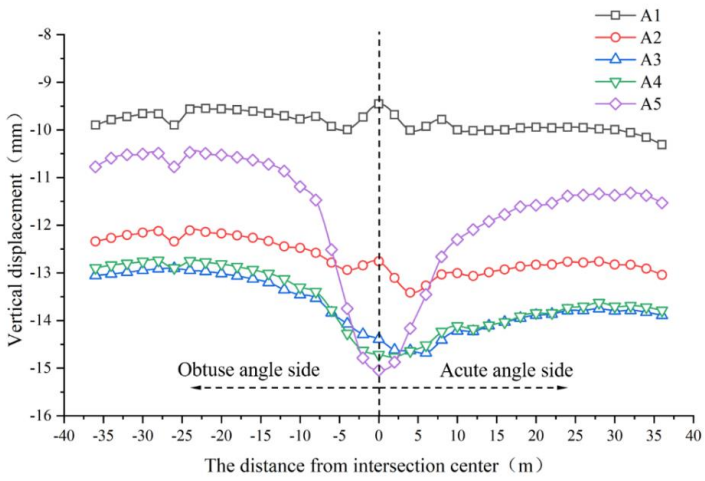

(a) The top of tunnel

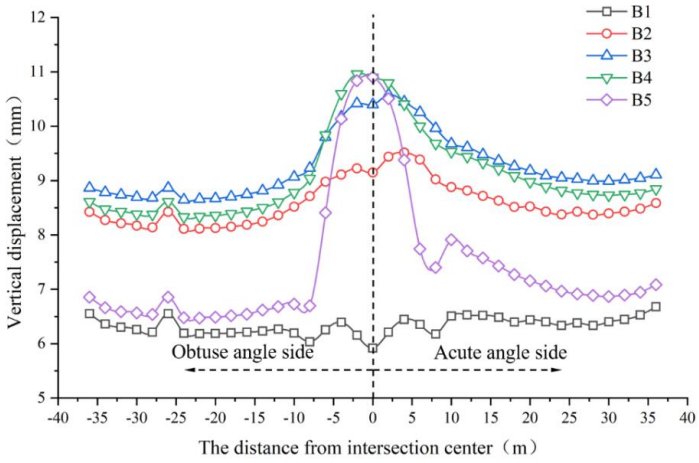

(b) The bottom of tunnel

Fig. 9 Variation curve of vertical displacement along tunnel axis

displacement of monitoring point A5 reaches about 15.2 mm, which is about 45% higher than the vertical displacement of monitoring point A5 at the section 30 m away from the intersection center. It can be found out from Fig. 9(b), the variation law of the vertical displacement at the bottom of the tunnel is consistent with that at the top of the tunnel. The monitoring point B5 is closest to the intersection area, so the variation of the vertical displacement is the largest. The maximum vertical displacement reaches about 10.8 mm, which is about 54% higher than that of the monitoring point B5 at the section 30 m away from the intersection center. The vertical displacement at the bottom of the tunnel is generally less than that at the top of the tunnel.

It can be found out from Fig. 10(a), the horizontal displacement distribution of each monitoring point on the left side of the tunnel is uniform, which is roughly symmetrically distributed about the intersection center. Moreover, the horizontal displacement of each monitoring point on the left side of the tunnel changes little along the axial direction of the tunnel. It can be seen that the surrounding rock on the left side of the tunnel is relatively stable and is less affected by the intersection area. Fig. 10(b) shows the variation curve of horizontal displacement on the right side of the tunnel along the tunnel axis. Due to the existence of the intersection area, the horizontal displacement values of monitoring points D2, D3, and D4 cannot be obtained within 6m from the intersection center section. It can be found out that the horizontal displacement distribution of each monitoring point on the right side of the tunnel is uneven. At the obtuse angle side, the horizontal displacement change of each monitoring point on the right side of the tunnel is relatively flat, and the horizontal displacement values of monitoring points D1 and D5 in the intersection area are small. At the acute angle side, the horizontal displacement change of each monitoring point on the right side of the tunnel is very obvious. With the increase of the distance from the intersection center, the horizontal displacement value of each monitoring line on the right side of the tunnel increases rapidly, and reaches the maximum value at about 16 m from the intersection center, and then the horizontal displacement value of each monitoring line on the right side of

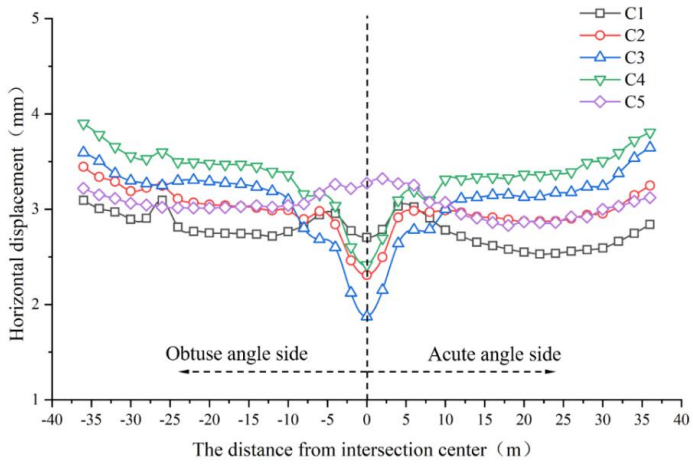

(a) The left side of tunnel

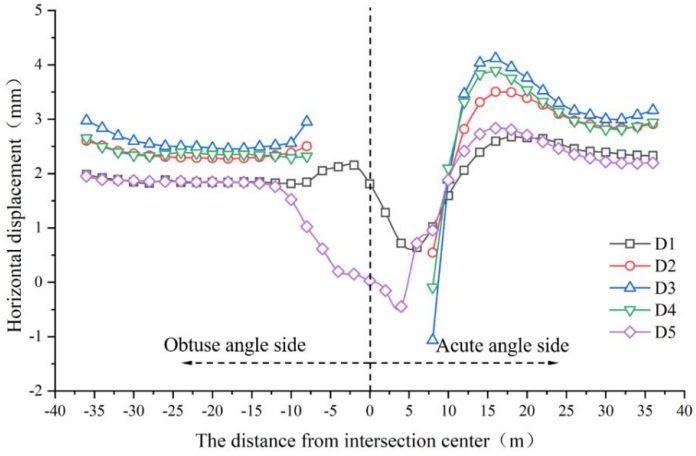

(b) The right side of tunnel

Fig. 10 Variation curve of horizontal displacement along tunnel axis

the tunnel gradually decreases. Among them, the horizontal displacement of monitoring line D3 changes most significantly. The maximum horizontal displacement of the monitoring line D3 is about 4.2 m, which is about 34% larger than the section 30m away from the intersection center. After 30 m from the intersection center, the horizontal displacement of each monitoring line tends to be stable.

At the section 8 m away from the intersection center at the acute angle side, the right side of the tunnel expands outward, which is because the rock mass between the construction adit and main tunnel is thin. After the excavation of the intersection section, the support structure on the right side of the main tunnel expands outward, and the rock mass at the included angle is offset to the direction of the construction tunnel. The displacement of rock mass leads to larger horizontal deformation of the construction adit section, and even destroys the supporting structure of the construction adit. This has been verified in engineering practice, as shown in Fig. 11. Therefore, the weak rock on the acute angle side of the intersection area needs additional reinforcement.

5.2 Influence of intersection angle between the main tunnel and construction adit on surrounding rock deformation

To study the influence of the intersection angle between the main tunnel and construction adit on the surrounding rock deformation, the excavation of five working conditions with intersection angle of 30˚, 45˚, 60˚, 75˚ and 90˚ is established. The calculation results of vault settlement and horizontal displacement of tunnels with different intersection angles are analyzed.

Fig. 12 shows the variation of vault settlement along the main tunnel axis at different intersection angles. It can be found out that the intersection angle has an obvious effect on the vault settlement. When the intersection angle is 30˚ ~ 60˚, the vault settlement on both sides of the intersection center is obviously asymmetric. Besides, the vault settlement on the acute angle side is larger than that on the obtuse angle side. The maximum settlement position of the arch crown is not at the intersection center, but on the acute angle side within 2 ~ 8 m

(a) The location of failure (b) The detail of the damage

Fig. 11 Failure of construction tunnel lining in the intersection area

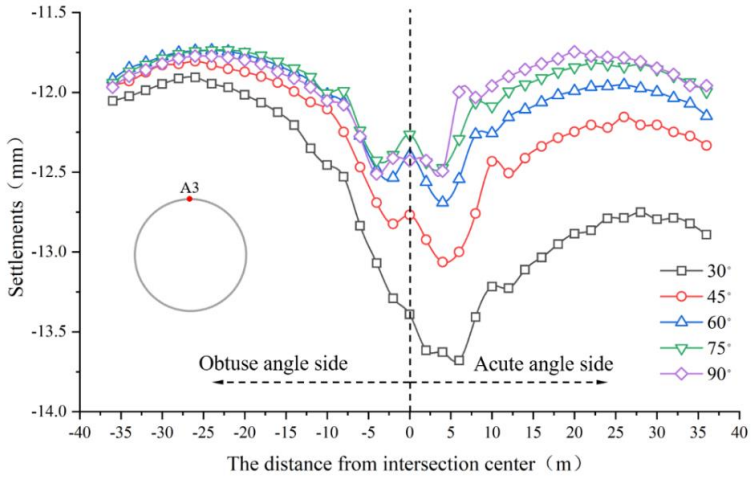

Fig. 12 Variation curve of arch crown settlement along the tunnel axis

to the intersection center. With the increase of the distance to the intersection center, the influence of the intersection area on the vault settlement decreases gradually. When the intersection angle is 75˚ ~ 90˚, the settlement value of the arch crown is symmetrically distributed about the intersection center. Besides, the settlement value of the arch crown at the intersection center is slightly larger than that on both sides. When the intersection angle is 30˚, the maximum settlement of the vault is about 13.7 mm, which is about 16% higher than the section 30 m away from the intersection center. When the intersection angle is 90˚, the maximum settlement of the vault is about 12.5 mm, which is only about 6% higher than the section 30 m away from the intersection center. It can be seen that the smaller the intersection angle, the greater the influence of it on the settlement.

Fig. 13 shows the variation of horizontal displacement along the main tunnel axis at different intersection angles. Fig. 13(a) is the horizontal displacement variation curve at monitoring point C3. Fig. 13(b) is the horizontal displacement variation curve at the monitoring point D3. Due to the existence of the intersection, monitoring point D3 cannot be arranged within 0 ~ 6 m from the intersection center, so the variation curve of monitoring point D3 is discontinuous. From the figure, it can be found out that the intersection angle has little effect on the horizontal displacement at monitoring point C3. The horizontal displacement value of monitoring point C3 is basically symmetrically distributed about the intersection center. The horizontal displacement at the intersection center is the smallest, and the horizontal displacement increases gradually with the increase of the distance to the intersection center. Compared with monitoring point C3, monitoring point D3 is affected obviously by the intersection angle. The maximum horizontal displacement of monitoring point D3 is at the acute angle side. With the increase of intersection angle, the maximum horizontal displacement of monitoring point D3 decreases gradually. The influence of crossing angle on the

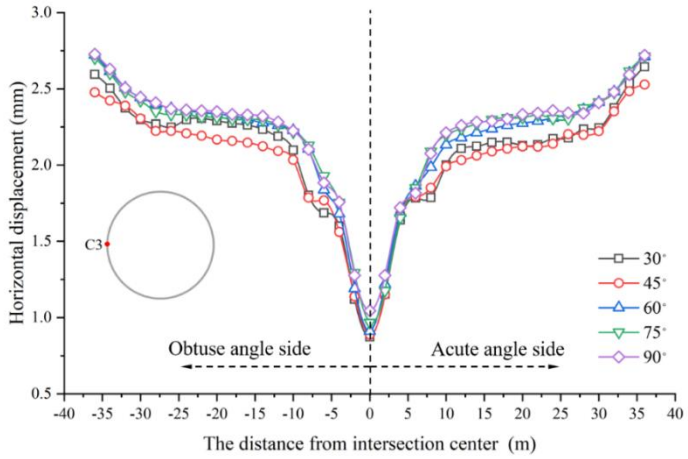

(a) Monitoring point C3

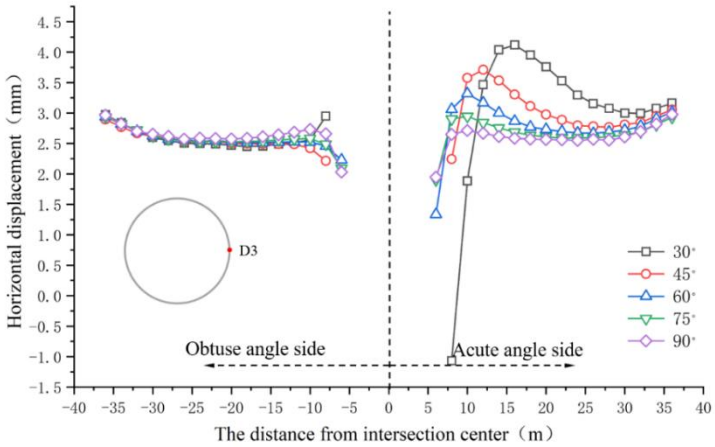

(b) Monitoring point D3

Fig. 13 Variation curve of horizontal displacement along the main tunnel axis

horizontal displacement of monitoring point D3 on the obtuse angle side is not significant.

5.3 Influence range of intersection area on surrounding rock deformation of the main tunnel

Although the deformation characteristics at different positions are different, the deformation at all positions tends to be stable at a certain distance to the intersection center. According to the numerical simulation results, the intersection angle between the main tunnel and construction adit has a significant impact on the surrounding rock deformation of the main tunnel. Therefore, the intersection angle must be considered to determine the influence range of the intersection area on the surrounding rock deformation. In addition, when the intersection angle is 30˚ ~ 60˚, the influence range at both sides of the intersection center is different, which needs to be explained separately. As can be seen from Figs. 12 and 13, with the increase of the intersection angle, the influence range of the intersection area is gradually reduced. When the intersection angle is 30˚, the influence range of the intersection area at the obtuse angle side is about 2B (B is the length of the main tunnel diameter), and the influence range at the acute angle side is about 2.5B. When the intersection angle is 60˚, the influence range at the obtuse angle side is about 1.5B, and the influence range at the acute angle side is about 2B. When the intersection angle is 90˚, the influence range at obtuse angle side and obtuse angle side is about 1.0B. The above results are consistent with the influence range results of Hsiao's study (Hsiao *et al.* 2009). The supporting structure of the tunnel within the influence range shall be strengthened.

6. Conclusions

In this paper, the Xianglushan tunnel of the water diversion project in central Yunnan Province is selected. The construction process of the intersection area is simulated by numerical simulation method. Combined with the field monitoring data, the spatial distribution characteristics of

surrounding rock deformation are analyzed. The construction models of tunnel intersection area with different intersection angles are established. The influence of intersection angle on the deformation of surrounding rock in the intersection is studied. The influence range of intersection area with different intersection angles is discussed. The following is the conclusion of this article:

(1) In general, after tunnel excavation, the deformation of surrounding rock in the vertical direction will be more significant, while the deformation of surrounding rock in the horizontal direction is relatively small. It can be seen from the numerical results that the vertical displacement value at the top of the tunnel > the vertical displacement value at the bottom of the tunnel > the horizontal displacement value at both sides of the tunnel for the same section.

(2) From the perspective of the axis of the main tunnel, the existence of the construction adit has a significant influence on the distribution characteristics of the deformation of the surrounding rock of the main tunnel, and the influence degree is related to the distance from the tunnel section to the intersection center. On both sides of the intersection center, the deformation of surrounding rock of the main tunnel in the range of -15 m~20 m from the intersection center is greatly affected by the construction adit. In this range, the vertical displacement on the top and bottom of the tunnel is larger, while the horizontal displacement on both sides of the tunnel is smaller. Outside the range of -15 m~20 m to the intersection center, the deformation of the surrounding rock of the main tunnel is basically not affected by the construction adit, and tends to be stable with the excavation of the tunnel.

(3) From the radial view of the main tunnel, the influence of the construction adit on the deformation of the surrounding rock at different locations of the main tunnel is obviously different. In the position close to the construction adit, the construction adit will have a greater impact on the surrounding rock of the main tunnel, and the deformation range is greater. In the position far away from the construction adit, the construction adit has little influence on the surrounding rock of the main tunnel, and the deformation range of the surrounding rock is small, which will not cause much change.

(4) The deformation of the surrounding rock of the tunnel on the obtuse side and the sharp side of the intersection area produces obvious non-uniformity and asymmetry characteristics. On the obtuse side of the intersection area, the deformation of the surrounding rock of the tunnel is small and the change amplitude is gentle. With the excavation of the tunnel, the deformation of the surrounding rock of the obtuse side of the tunnel becomes stable faster. In the intersection area, the deformation of the surrounding rock of the tunnel is large and the change range is also large, and the construction adit has a greater influence on the deformation of the surrounding rock.

(5) The intersection angle between the main tunnel and construction adit has a significant impact on the surrounding rock deformation. The smaller the intersection angle is, the larger the deformation of surrounding rock is. Besides, the deformation distribution on both sides of the intersection is obviously asymmetric when the intersection angle is smaller than 60°. Therefore, a larger intersection angle is more conducive to the stability of surrounding rock in the intersection area. The influence range of the intersection on the surrounding rock deformation is related to the intersection angle between the main tunnel and construction adit. The larger the intersection angle is, the smaller the influence range is. It is suggested to reinforce the supporting structure and strengthen the deformation monitoring within the influence range.

There are some limitations in this paper:(1) In order to simplify the calculation process, the uniformity assumption (Mohr-Coulomb model) of surrounding rock properties is made in the numerical simulation in this paper. However, there are many changes in the properties and structures of surrounding rock in actual engineering, so there are some errors between the numerical calculation results and the field test results. In the future, it is necessary to conduct strict simulation of surrounding rock structure, so as to reflect the deformation characteristics of surrounding rock in the intersection area more accurately. (2) This paper only considers the influence of intersection angle on the deformation of surrounding rock in the intersection area, and the diameter ratio between the construction adit and the main tunnel is approximately 0.60. Other factors affecting the deformation of surrounding rock in the intersection area need to be further studied; (3) The deformation of surrounding rock in the intersection area is affected by many factors, and each factor is also correlated with each other. In the future, more influential factors will be further studied and the correlation analysis of influential factors will be carried out to establish a more perfect and reasonable evaluation system for surrounding rock deformation in the intersection area. (4) The research is based on the engineering practice of Xianglushan Tunnel, which inevitably has certain regional characteristics and has certain reference value for similar projects, and is not applicable to all engineering practices. In the future, the model will be established and optimized more reasonably according to the continuous enrichment of engineering cases.

Acknowledgments

We would like to acknowledge the financial support from the National Natural Science Foundation of China (Grant Nos.: 42172310, 51609130, 41977222, 42007234), and the Youth Innovation Technology Project of Higher School in Shandong Province (2019KJG015).

References

Budarapu, P. R., Narayana, T.S.S., Rammohan, B. and Rabczuk, T. (2015), "Directionality of sound radiation from rectangular panels", *Appl. Acoust.*, **89**, 128-140. https://doi.org/10.1016/j.apacoust.2014.09.006.

Budarapu, P.R., Yb, S.S., Javvaji, B. and Mahapatra, D.R. (2014), "Vibration analysis of multi-walled carbon nanotubes embedded in elastic medium", *Front. Struct. Civil Eng.*, **8**(2), 151-159. https://doi.org/10.1007/s11709-014-0247-9.

Chen, C.N. and Tseng, C.T. (2010), "2D tunneling chart from redistributed 3D principal stress path", *Tunn. Undergr. Sp. Tech.*, **25**(4), 305-314. https://doi.org/10.1016/j.tust.2010.01.003.

Chen, L.A., Pei, W.W., Yang, Y.H. and Guo, W.L. (2022), "Three-

dimensional numerical parametric study of shape effects on multiple tunnel interactions", *Geomech. Eng.*, **31**(3), 237-248. https://doi.org/10.12989/gae.2022.31.3.237.

Chortis, F. and Kavvadas, M. (2021), "Three-dimensional numerical analyses of perpendicular tunnel intersections", *Geotech. Geol. Eng.*, **39**, 1771-1793. https://doi.org/10.1007/s10706-020-01587-w.

Dong, L., Zhong, S. and Wang, H.L. (2020), "Dynamic response characteristics of crossing tunnels under heavy-haul train loads", *Geomech. Eng.*, **20**(2), 103-112. https://doi.org/10.12989/gae.2020.20.2.103.

Elkadi, A.S. and Huisman, M. (2002), "3D-GSIS geotechnical modelling of tunnel intersection in soft ground: the Second Heinenoord Tunnel, Netherlands", *Tunn. Undergr. Sp. Tech.*, **17**(4), 363-369. https://doi.org/10.1016/S0886-7798(02)00039-1.

Fan, Y., Zheng, J.W., Cui, X.Z., Leng, Z., Wang, F. and Lv, C. (2021), "Damage zones induced by in situ stress unloading during excavation of diversion tunnels for the Jinping II hydropower project", *Bull. Eng. Geol. Environ.*, **80**, 4689-4715. https://doi.org/10.1007/s10064-021-02172-y.

Gerçek, H. (1986), "Stability considerations for underground excavation intersections", *Min. Sci. Tech.*, **4**(1), 49-57. https://doi.org/10.1016/S0167-9031(86)90194-5.

Hsiao, F.Y., Wang, C.L. and Chern, J.C. (2009), "Numerical simulation of rock deformation for support design in tunnel intersection area", *Tunn. Undergr. Sp. Tech.*, **24**(1), 14-21. https://doi.org/10.1016/j.tust.2008.01.003.

Jiang, Y., Zhou, H., Lu, J., Gao, Y., Zhang, C. and Chen, J. (2019), "Analysis of stress evolution characteristics during TBM excavation in deep buried tunnels", *Bull. Eng. Geol. Environ.*, **78**, 5177-5194. https://doi.org/10.1007/s10064-019-01466-6.

Johnson, R.L. and Leven, M.M. (1977), "Stress-concentration factors at intersecting and closely approaching orthogonal coplanar holes", *Exp. Mech.*, **17**(1), 1-6. https://doi.org/10.1007/BF02324264.

Joneidi, M., Golshani, A. and Naeimifar, I. (2019), "Progressive deformation and mechanical behaviour of intersecting tunnels in soft ground", *Proceedings of the Institution of Civil Engineers-Ground Improvement*, **172**(4), 285-296. https://doi.org/10.1680/jgrim.18.00073.

Li, X., Xue, Y., Qiu, D., Ma, X., Qu, C., Zhou, B. and Kong, F. (2021), "Application of data mining to lagging deformation prediction of the underwater shield tunnel", *Mar. Georesour. Geotech.*, **39**(2), 163-175. https://doi.org/10.1080/1064119X.2019.1681039.

Li, Y., Jin, X., Lv, Z., Dong, J. and Guo, J. (2016), "Deformation and mechanical characteristics of tunnel lining in tunnel intersection between subway station tunnel and construction tunnel", *Tunn. Undergr. Sp. Tech.*, **56**, 22-33. https://doi.org/10.1016/j.tust.2016.02.016.

Li, Y., Qi, T., Lei, B., Qian, W. and Li, Z. (2019), "Deformation patterns and surface settlement trough in stratified jointed rock in tunnel excavation", *KSCE J. Civil Eng.*, **23**(7), 3188-3199. https://doi.org/10.1007/s12205-019-0477-4.

Liang, Z., Xue, R., Xu, N. Dong, L. and Zhang, Y. (2020), "Analysis on microseismic characteristics and stability of the access tunnel in the main powerhouse, Shuangjiangkou hydropower station, under high in situ stress", *Bull. Eng. Geol. Environ.*, **79**, 3231-3244. https://doi.org/10.1007/s10064-020-01738-6.

Lin, P., Zhou, Y., Liu, H. and Wang, C. (2013), "Reinforcement design and stability analysis for large-span tailrace bifurcated tunnels with irregular geometry", *Tunn. Undergr. Sp. Tech.*, **38**, 189-204. https://doi.org/10.1016/j.tust.2013.07.011.

Liu, H.L., Li, S.C., Li, L.P. and Zhang, Q.Q. (2017), "Study on deformation behavior at intersection of adit and major tunnel in railway", *KSCE J. Civil Eng.*, **21**(6), 2459-2466. https://doi.org/10.1007/s12205-017-2128-y.

Liu, H., Li, P. and Liu, J. (2011), "Numerical investigation of underlying tunnel heave during a new tunnel construction", *Tunn. Undergr. Sp. Tech.*, **26**(2), 276-283. https://doi.org/10.1016/j.tust.2010.10.002.

Liu, X. and Wang, Y. (2010), "Three dimensional numerical analysis of underground bifurcated tunnel", *Geotech. Geol. Eng.*, **28**(4), 447-455. https://doi.org/10.1007/s10706-010-9304-x.

Luo, Y., Chen, J., Wang, H. and Sun, P. (2017), "Deformation rule and mechanical characteristics of temporary support in soil tunnel constructed by sequential excavation method", *KSCE J. Civil Eng.*, **21**(6), 2439. https://doi.org/10.1007/s12205-016-0978-3.

Nawel, B. and Salah, M. (2015), "Numerical modeling of two parallel tunnels interaction using three-dimensional Finite Elements Method", *Geomech. Eng.*, **9**(6), 775-791. https://doi.org/10.12989/gae.2015.9.6.775.

Riley, W.F. (1964), "Stresses at tunnel intersections", *J. Eng. Mech. Division*, **90**(2), 167-179. https://doi.org/10.1061/JMCEA3.0000464.

Shi, J.W., Wang, J.P., Ji, X.J., Liu, H.Q. and Lu, H. (2022), "Three-dimensional numerical parametric study of tunneling effects on existing pipelines", *Geomech. Eng.*, **30**(4), 383-392. https://doi.org/10.12989/gae.2022.30.4.383.

Shi, J., Ng, C.W.W. and Chen, Y. (2015), "Three-dimensional numerical parametric study of the influence of basement excavation on existing tunnel", *Comput. Geotech.*, **63**, 146-158. https://doi.org/10.1016/j.compgeo.2014.09.002.

Song, D., Liu, X., Chen, Z., Chen, J. and Cai, J. (2021), "Influence of tunnel excavation on the stability of a bedded rock slope: A case study on the mountainous area in Southern Anhui, China", *KSCE J. Civil Eng.*, **25**(1), 114-123. https://doi.org/10.1007/s12205-020-0831-6.

Sudhir Sastry, Y.B., Budarapu, P.R., Krishna, Y. and Devaraj, S. (2014), "Studies on ballistic impact of the composite panels", *Theor. Appl. Fract. Mech.*, **72**, 2-12. https://doi.org/10.1016/j.tafmec.2014.07.010.

Sudhir Sastry, Y.B., Budarapu, P.R., Madhavi, N. and Krishna, Y. (2015), "Buckling analysis of thin wall stiffened composite panels", *Comput. Mater. Sci.*, **96**, 459-471. https://doi.org/10.1016/j.commatsci.2014.06.007.

CC